Langmuir
Article
pubs.acs.org/Langmuir

Influence of Surface Oxides on the Colloidal Stability of Multi-Walled Carbon Nanotubes: A Structure−Property Relationship

Billy Smith,[†] Kevin Wepasnick,[†] Kaitlin E. Schrote,[‡] Hyun-Hee Cho,[§] William P. Ball,[§] and D. Howard Fairbrother*,[†,∥]

[†]*Department of Chemistry, The Johns Hopkins University, Baltimore, Maryland 21218,* [‡]*Department of Chemistry, College of Notre Dame of Maryland, Baltimore, Maryland,* [§]*Department of Geography and Environmental Engineering, The Johns Hopkins University, Baltimore, Maryland 21218, and* [∥]*Department of Materials Science and Engineering, The Johns Hopkins University, Baltimore, Maryland 21218*

Received March 31, 2009. Revised Manuscript Received June 13, 2009

As with all nanomaterials, a large fraction of the atoms in carbon nanotubes (CNTs) reside at or near the surface. Consequently, surface chemistry will play a crucial role in determining the fate and transport of CNTs in aquatic environments. Frequently, oxygen-containing functional groups (surface oxides) are deliberately grafted into the CNT surface to promote colloidal stability. To study the influence that both the oxygen concentration and the oxygen functional-group distribution have on the colloidal stability of multiwalled carbon nanotubes (MWCNTs), a suite of oxidized MWCNTs (O-MWCNTs) were created using different oxidizing agents and reaction conditions. Stable colloidal suspensions were prepared by low-power sonication of O-MWCNT powders in Milli-Q water. Results from TEM, AFM, DLS, and XPS measurements revealed that, irrespective of the surface chemistry, the colloidal suspensions were composed of individual nanotubes with comparable length distributions. The critical coagulation concentrations (CCC) of O-MWCNTs that exhibited different surface chemistries were measured with time-resolved dynamic light scattering (TR-DLS) using NaCl as the electrolyte. Over a range of environmentally relevant pH values, linear correlations were found to exist between the CCC, total oxygen concentration, and surface charge of O-MWCNTs. In contrast to surface charge, electrophoretic mobility did not prove to be a useful metric of colloidal stability. Information obtained from chemical derivatization studies, carried out in conjunction with XPS, revealed that the distribution of oxygen-containing functional groups also influences the colloidal stability of O-MWCNTs, with carboxylic acid groups playing the most important role. This study highlights the fact that quantitative relationships can be developed to rationalize the influence of surface chemistry on the behavior of nanomaterials in aquatic environments.

(I). Introduction

Over the past several years, the number of technologies and consumer products that incorporate engineered nanomaterials has grown rapidly with corresponding increases in their annual production rates.[1] Inevitably, some of these synthetic nanomaterials will enter the environment either from incidental release during manufacture and transport or following consumer use and disposal. Currently, little is known about the ecological behavior and impact of these materials,[2−5] and as a result, intense scientific research is now being directed toward understanding the health and safety risks posed by different types of engineered nanomaterials.[3,5−9] One systematic and scientifically rigorous approach to improve our understanding is to develop functional relationships between fundamental materials properties (e.g., size, shape and composition) and environmentally relevant behaviors, such as colloidal stability, sorption properties, and toxicity. In this respect, surface chemistry is expected to play a pivotal role in determining a nanomaterial's behavior because the majority of the atoms are located at or near the surface.[10−13]

In aquatic environments, changes in a nanomaterial's surface composition can occur as a result of either chemical reactions or the physisorption of biological macromolecules or surfactants.[14,15] In either case, the nanomaterial's surface charge and surface potential (zeta potential) will change, altering not only the interactions between individual nanoparticles but also their interactions with surrounding water molecules. For example, the presence of surface-bound hydroxyl groups is responsible for pronounced differences in the aquatic stability, mobility, and aggregation state of fullerols relative to fullerenes.[16,17] Similarly,

*To whom correspondence should be addressed. E-mail: howardf@jhu.edu.

(1) Short, P.; McCoy, M. *Chem. Eng. News* **2007**, *85*, (37), 20.
(2) Owen, R.; Handy, R. *Environ. Sci. Technol.* **2007**, 5582−5588.
(3) Wiesner, M. R.; Lowry, G. V.; Alvarez, P.; Dionysiou, D.; Biswas, P. *Environ. Sci. Technol.* **2006**, 4336−4345.
(4) Dionysiou, D. D. *J. Environ. Eng.* **2004**, *130*, (7), 723−724.
(5) Handy, R. D.; Owen, R.; Valsami-Jones, E. *Ecotoxicology* **2008**, *17*, 315−325.
(6) Maynard, D. A. *Nature* **2006**, *444*, 267−269.
(7) Guzman, K. A. D.; Taylor, M. R.; Banfield, J. F. *Environ. Sci. Technol.* **2006**, *40*, 1401−1407.
(8) Oberdorster, G.; Oberdorster, E.; Oberdorster, J. *Environ. Health Perspect.* **2005**, *13*, 823−840.
(9) Klaine, S. J.; Alvarez, P. J. J.; Batley, G. E.; Fernandes, T. F.; Handy, R. D.; Lyon, D. Y.; Mahendra, S.; McLaughlin, M. J.; Lead, J. R. *Environ. Toxicol. Chem.* **2008**, *27*, 1825−1851.
(10) Christian, P.; Kammer, F. V. d.; Baalousha, M.; Hofmann, T. *Ecotoxicology* **2008**, *17*, 326−343.
(11) Sayes, C. M.; Liang, F.; Hudson, J. L.; Mendez, J.; Guo, W.; Beach, J. M.; Moore, V. C.; Doyle, C. D.; West, J. L.; Billups, W. E.; Ausman, K. D.; Colvin, V. L. *Toxicol. Lett.* **2006**, *161*, 135−142.
(12) Bottini, M.; Bruckner, S.; Nita, K.; Bottini, N.; Belluci, S.; Magrini, A.; Bergamaschi, A.; Mustelin, T. *Toxicol. Lett.* **2006**, *160*, 121−126
(13) Arias, L. R.; Yang, L. *Langmuir* **2009**, *25*, 3003−3012.
(14) Fortner, J. D.; Kim, D.; Boyd, A. M.; Falkner, J. C.; Moran, S.; Colvin, V. L.; Hughes, J. B.; Kim, J.-H. *Environ. Sci. Technol.* **2007**, *41*, 7497−7502.
(15) Hyung, H.; Fortner, J. D.; Hughes, J. B.; Kim, J.-H. *Environ. Sci. Technol.* **2007**, *41*, 179−184.
(16) Lecoanet, H. F.; Bottero, J.-Y.; Wiesner, M. R. *Environ. Sci. Technol.* **2004**, *38*, (19), 5164−5169.
(17) Lecoanet, H. F.; Wiesner, M. R. *Environ. Sci. Technol.* **2004**, *38*, 4377−4382.

the adsorption of natural organic matter or synthetic surfactants has been shown to alter the colloidal stability of both naturally occurring and engineered nanoparticles (e.g., hematite and carbon nanotubes).[15,18−20]

By changing the forces between nanoparticles and the stationary materials (e.g., sand and hematite) with which they collide, surface chemistry will also influence the transport properties of colloidal nanoparticles in the environment.[21−28] For example, the transport properties of polymer-coated nanoscale zero valent iron (NZVI) are influenced by the chemical composition of the polymer coating.[29] Surface chemistry will also impact a nanomaterial's ability to sorb other species present in the environment and in this regard, changes in surface chemistry have recently been shown to strongly influence the sorption properties of nanoparticles toward hydrophobic organic chemicals and transition metal cations.[30−38] Furthermore, since interfacial properties regulate both sorption and transport, changes in surface chemistry will have important implications for the ability of an engineered nanomaterial to act as a so-called "Trojan Horse," facilitating the transport of toxins.[39]

Stable colloidal suspensions of CNTs are needed in an increasing number of existing and projected applications, including polymer composites[37,38] and drug delivery agents.[39−42] In the absence of surface modification, pristine CNTs fail to form stable colloidal suspensions, even after prolonged sonication. To prepare uniform, well-dispersed mixtures, the CNTs' exterior surface must first be modified. One of the most prevalent surface modification techniques involves grafting hydrophilic oxygen-containing functional groups (surface oxides) into the exterior graphene sheet, using strong oxidizing agents (e.g., HNO_3, HNO_3/H_2SO_4, O_3, $KMnO_4$ or H_2O_2). Indeed, colloidally stable dispersions of acid-washed CNTs are now commercially available. It should also be noted that even when aqueous dispersions are not the ultimate objective, these same highly oxidizing conditions are frequently used to remove amorphous carbon and metallic impurities from commercially available CNTs. To disperse the surface modified CNTs, bath or probe sonication are commonly used. Both methods provide the energy needed to overcome the attractive van der Waals forces between individual CNTs and disentangle them from aggregates. During the sonication period, physical and chemical changes to the CNT may occur.[40,41]

In the present study, we focus on the effect that surface-bound, oxygen-containing functional groups have on the aqueous colloidal stability of multiwalled carbon nanotubes (MWCNTs). We have examined MWCNTs rather than SWCNTs because the annual production rate of MWCNTs is currently three to four times that of SWCNTs.[42] The surface properties of oxidized MWCNTs (O-MWCNTs) were characterized using a combination of X-ray photoelectron spectroscopy, chemical derivitization, electrophoretic mobility, and surface charge measurements. The colloidal stability of dispersed O-MWCNT particles were examined under different aquatic conditions (pH and electrolyte concentration) using time-resolved dynamic light scattering (TR-DLS).[18−20,43−47] This investigation builds on methods developed in previous studies which showed that many of the mathematical models and equations developed to describe the aggregation kinetics and colloidal properties of spherical particles could also be applied to model the behavior of rod-like CNTs under different aquatic conditions.[47,48] Specifically, the behavior of acid-washed CNTs in aquatic environments has been shown to adhere to the basic precepts of DLVO theory.[47−49]

A central goal of this study was to see if fundamental CNT properties (i.e., surface composition, electrophoretic mobility, or surface charge) could be correlated with a phenomenological behavior (i.e., colloidal stability) that will have a more direct impact on the environmental fate and effect of O-MWCNTs. This has been accomplished by studying the colloidal properties of different O-MWCNTs prepared using common oxidants and reaction conditions, coupled with detailed information on their surface properties.

(II). Experimental Section

Preparation of Oxidized MWCNTs (O-MWCNTs). Pristine MWCNTs were purchased from NanoLab Inc. (outer diameters 15 ± 5 nm, lengths 5−20 μm). As-received MWCNTs contained >95% carbon by weight. To achieve this level of purity, the manufacturer treated the MWCNTs with HF/HCl to remove most of the residual Fe or Ni catalyst particles used to grow the MWCNTs.

In this study, three different acid-washing treatments were used to oxidize the pristine MWCNTs: Nitric acid (HNO_3), potassium permagnate ($KMnO_4$), and sulfuric acid/nitric acid (H_2SO_4/HNO_3). Oxidative treatments using HNO_3 and $KMnO_4$ were conducted at Johns Hopkins University; oxidative treatments using H_2SO_4/HNO_3 were performed by Nanolabs Inc.

HNO_3. Following methods described by Cho et al.,[30] MWCNTs (100 mg) were initially dispersed for 1 h by sonication (Branson 1510, operating at 70 W) in 250 mL of HNO_3. After

(18) Chen, K. L.; Mylon, S. E.; Elimelech, M. *Langmuir* **2007**, *23*, 5920−5928.
(19) Chen, K. L.; Elimelech, M. *J. Colloid Interface Sci.* **2007**, *309*, 126−134.
(20) Mylon, S. E.; Chen, K. L.; Elimelech, M. *Langmuir* **2004**, *20*, 9000−9006.
(21) O'Melia, C. R. *Colloids Surf.* **1989**, *39*, 255−271.
(22) Elimelech, M.; O'Melia, C. R. *Environ. Sci. Technol.* **1990**, *24*, 1528−1536.
(23) Franchi, A.; O'Melia, C. R. *Environ. Sci. Technol.* **2003**, *37*, 1122−1129.
(24) Kretzschmar, R.; Borkovec, M.; Grolimund, D.; Elimelech, M. *Adv. Agronomy* **1999**, *66*, 121−193.
(25) Grolimund, D.; Elimelech, M.; Borkovec, M. *Colloids Surf. A* **2001**, *191*, 179−188.
(26) Saleh, N.; Kim, H.-J.; Matyjaszewski, K.; Tilton, R. D.; Lowry, G. V. *Environ. Sci. Technol.* **2008**, *42*, 3349−3355.
(27) Espinasse, B.; Hotze, E. M.; Wiesner, M. R. *Environ. Sci. Technol.* **2007**, *41*, 7396−7402.
(28) Zhan, J.; Zheng, T.; Piringer, G.; Day, C.; L., M. G.; Lu, Y.; Papadopoulos, K.; John, V. T. *Environ. Sci. Technol.* **2008**, *42*, 8871−8876.
(29) Phenrat, T.; Long, T. C.; Lowry, G. V.; Veronesi, B. *Environ. Sci. Technol.* **2009**, *43*, 195−200.
(30) Cho, H.-H.; Smith, B. A.; Wnuk, J.; Fairbrother, H.; Ball, W. P. *Environ. Sci. Technol.* **2008**, *42*, 2899−2905.
(31) Cho, H.-H.; Wepasnick, K.; Smith, B. A.; Fairbrother, D. H.; Ball, W. P. *Langmuir*, in preparation.
(32) Bond, A. M.; Miao, W.; Raston, C. L. *Langmuir* **2000**, *16*, 6004−6012.
(33) Li, Y.-H.; Wang, S.; Wei, J.; Zhang, X.; Xu, C.; Luan, Z.; Wu, D.; Wei, B. *Chem. Phys. Lett.* **2002**, *357*, 263−266.
(34) Li, Y. H.; Ding, J.; Luan, Z. K.; Di, Z. C.; Zhu, Y. F.; Xu, C. L.; Wu, D. H.; Wei, B. Q. *Carbon* **2003**, *41*, (14), 2787−2792.
(35) Lubick, N. *Environ. Sci. Technol.* **2008**, 1821−1824.
(36) Wang, X.; Chen, C. *Ind. Eng. Chem. Res.* **2006**, *45*, 9144−9149.
(37) Lu, C.; Chiu, H. *Chem. Eng. Sci.* **2006**, *61*, 1138−1145.
(38) Lu, C.; Chiu, H.; Liu, C. *Ind. Eng. Chem. Res.* **2006**, *45*, 2850−2855.
(39) Limbach, L. K.; Wick, P.; Manser, P.; Grass, R. N.; Bruinink, A.; Stark, W. J. *Environ. Sci. Technol.* **2007**, *41*, (11), 4158−4163.
(40) Hennrich, F.; Krupke, R.; Arnold, K.; Rojas Stutz, J. A.; Lebedkin, S.; Koch, T.; Schimmel, T.; Kappes, M. M. *J. Phys. Chem. B* **2007**, *111*, (8), 1932−1937.
(41) Yang, D.-Q.; Rochette, J.-F.; Sacher, E. *J. Phys. Chem. B* **2005**, *109*, 7788−7794.
(42) CientificaNanotubes , http:// www.cientifica.com/www/summarys/Nanotubes_2004_ExSum.pdf., 2004.
(43) Chen, K. L.; Mylon, S. E.; Elimelech, M. *Environ. Sci. Technol.* **2006**, *40*, 1516−1523.
(44) Chen, K. L.; Elimelech, M. *Langmuir* **2006**, *22*, 10994−11001.
(45) He, Y. T.; Wan, J.; Tokunaga, T. *J. Nanopart. Res.* **2008**, *10*, 321−332.
(46) Phenrat, T.; Saleh, N.; Sirk, K.; Tilton, R. D.; Lowry, G. V. *Environ. Sci. Technol.* **2007**, *41*, 284−290.
(47) Saleh, N. B.; Pfefferle, L. D.; Elimelech, M. *Environ. Sci. Technol.* **2008**, *42*, (21), 7963−7969.
(48) Smith, B.; Wepasnick, K.; Schrote, K. E.; Bertele, A. R.; Ball, W. P.; O'Melia, C.; Fairbrother, D. H. *Environ. Sci. Technol.* **2009**, *43*, 819−825.
(49) Sano, M.; Okamura, J.; Shinkai, S. *Langmuir* **2001**, *17*, 7172−7173.

sonication, the MWCNT-HNO_3 mixture was refluxed at 140 °C for 1.5 h while stirring vigorously; after which time, it was allowed to cool to room temperature. To vary the oxidative power in these preparations, HNO_3 concentrations in the refluxing solution were varied between 0% and 70% w/w. This range of HNO_3 concentrations was chosen to mimic the range of conditions used by researchers for acid-washing or purifying CNTs.[36,50−52]

$KMnO_4$. Following the procedure outlined by Hiura et al.,[53] MWCNTs (100 mg) were sonicated in 200 mL of H_2SO_4 (1.0 N) for 30 min. To a separate flask, $KMnO_4$ (250 mg) was dissolved in 200 mL of H_2SO_4 (1.0 N). After sonication, the MWCNT suspension was heated to 150 °C, and the $KMnO_4$ solution was added dropwise. The mixture was reflux for 5 h; after which time, it was allowed to cool to room temperature. Before the oxidized MWCNTs were extracted, 10 mL of concentrated HCl was added to remove the Mn-containing byproducts by forming insoluble complexes.

H_2SO_4/HNO_3. At Nanolabs Inc., O-MWCNTs were prepared by mixing the pristine nanotubes with a 3:1 mixture of concentrated $H_2SO_4-HNO_3$ (~12.5 mg of MWCNT to 1 mL H_2SO_4:HNO_3). Oxidation was accomplished using two different reaction conditions: in one, the $H_2SO_4-HNO_3$ MWCNT mixture was refluxed at 70 °C for 8 h, while in the other method, the mixture was microwaved ($\mu\lambda/H_2SO_4-HNO_3$).

O-MWCNT Purification. As described in Smith et al.[48] O-MWCNTs were extracted from the residual acids, metallic byproducts, and amorphous carbon by repeated cycles of dilution with Milli-Q water, centrifugation (Powerspin LX, Unico), and decanting the solutions until the resistivity of the supernatant was greater than 0.5 MΩ and the pH was ≈5. O-MWCNTs were then dried overnight in an oven at 100 °C. Once dry, the O-MWCNT powders were pulverized in a ball-mill (MM200, Retsch) for 15 min.

Characterization of O-MWCNTs. *Surface Characterization*. X-ray photoelectron spectroscopy was used to quantify the extent of MWCNT surface oxidation as described in Cho et al.[30] To ensure consistency in our XPS analysis, O-MWCNT powders were adhered to a 1 cm × 1 cm piece of double-sided copper tape and analyzed using a 2.8 mm analysis area. Carbon and oxygen were the only two elements observed during XPS analysis.

Vapor phase chemical derivatization was used to quantify the distribution of carboxyl (COOH), hydroxyl (C−OH), and carbonyl (C═O) groups on the surface of O-MWCNTs as described in detail in Langley et al.[54,55] In these experiments, a fluorine containing labeling reagent (trifluoroacetic anhydride, trifluoroethanol, or trifluoroethyl hydrazine) is used that reacts selectively with one oxygen-containing functional group (hydroxyl, carboxylic acid, and carbonyl groups, respectively). After each derivatization reaction, the F(1s) signal can be used to quantify the concentration of the targeted surface oxide on the O-MWCNT.[54,55]

To complement our XPS and chemical derivitization data, the surface-charge density on the majority of the O-MWCNTs studied was determined by potentiometric titration. In these experiments, a known mass of O-MWCNTs was dispersed by sonication for 10 min in a known volume of Milli-Q water. The suspension was then transferred to a titration apparatus which was isothermally controlled (25 °C) and sparged with nitrogen. Before each titration, the pH was adjusted to ~4 using 0.02 M HCl, and the ionic strength was set to ~64 mM with NaCl. The solution was then titrated with 20 μL aliquots of 0.02 M NaOH; after each aliquot was added, the pH was allowed to reach equilibrium. The O-MWCNTs′ charge as a function of pH was calculated by solving the following charge balance eq 1:

$$[\text{O-MWNCT}]_{\text{charge}} = [Cl^-]+[OH^-]-[H^+]-[Na^+] \quad (1)$$

The surface charge density of each O-MWCNT was calculated using the Brunauer−Emmett−Teller (BET) surface areas (ASAP 2000, Micometrics Corp.) reported in Supporting Information, Table S1.

Preparation of Colloidal O-MWCNT Stock Solutions. To prepare stable colloidal suspensions, a known mass (< 600 μg) of O-MWCNTs was sonicated in 200 mL of Milli-Q water for 20 h (Branson 1510, operating at 70 W). For those O-MWCNTs that could form stable suspensions, this sonication time represented the minimum period required to disperse the MWCNTs such that no visible aggregates were observable, either in solution, at the air/water interface, or on the walls or bottom of the container. After sonication, the pH was adjusted to 4, 6, or 8 using various buffers: pH 4 (20 μL/1 M $CH_3COOH/NaCH_3COO$); pH 6 (100 μL/1 M $CH_3COOH/NaCH_3COO$); pH 8 (200 μL/0.1 M $NaHCO_3/Na_2CO_3$). We have shown previously that the presence of acetate buffers in solution does not influence the colloidal properties of O-MWCNTs.[48] After addition of the buffer, the colloidal suspension was sonicated for an additional hour. Undesirable particles such as dust, glass etched during sonication, and some larger CNT bundles were removed by centrifugation (5 min, 3000 rpm). The pH was then readjusted by adding NaOH or HCl as needed.

Characterization of Colloidal O-MWCNTs. *Electrophoretic Mobility*. The electrophoretic mobility of colloidally dispersed particles was determined for each O-MWCNT suspension (concentration~ 4.8 mg/L) as a function of pH at constant ionic strength (I = 64) using a capillary cell method (Zetasizer-3000HSa, Malvern Instruments). To remove any dust and residual macroscopic particles, NaCl solutions and Milli-Q water were filtered though a 0.2 μm PES syringe filter. For each solution condition, 10 electrophoretic mobility measurements were performed. To verify the accuracy of the instrument, reference experiments were conducted on polystyrene latex standard particles (Part-#:DTS1050) provided by Malvern Instruments Ltd. Our measured values (−50 ± 3 mV) were in excellent agreement with the reference values (−50 ± 5 mV).

Length Distribution. The length distributions of selected O-MWCNT suspensions were evaluated with Atomic Force Microscopy (AFM: Pico SPM LE, Agilent). To preserve the aggregation state upon drying, colloidal suspensions (4.6 mg O-MWCNTs/L) were misted and flash deposited onto a heated, atomically smooth silicon substrate, using a laboratory spray bottle equipped with an atomizer. A sufficient number of 11.4 μm × 11.4 μm AFM images were then acquired and analyzed to determine the length of O-MWCNTs.

Structure. For selected O-MWCNTs, the structure of colloidally dispersed particles was examined using transmission electron microscopy (TEM). TEM samples were prepared by dipping a holey-carbon TEM grid into a colloidal suspension of the MWCNTs. Imaging was accomplished using a Philips CM 300 field emission gun transmission electron microscope operating at 297 kV. Images were collected using a CCD camera mounted on a GIF 200 electron energy loss spectrometer.

Colloidal Stability. The colloidal stability of O-MWCNTs was assessed by monitoring their early time aggregation rates as a function of electrolyte (NaCl) concentration using time-resolved dynamic light scattering (TR-DLS, Brookhaven Instruments). All NaCl solutions and Milli-Q water used in TR-DLS experiments were filtered though a 0.2 μm PES syringe filter. DLS experiments were carried out at 25 °C using an Ar ion laser (488 nm) operating

(50) Martinez, M. T.; Callejas, M. A.; Benito, A. M.; Cochet, M.; Seeger, T.; Anson, A.; Schreiber, J.; Gordon, C.; Marhic, C.; Chauvet, O.; Maser, W. K. *Nanotechnology* **2003**, *14*, 691−695.
(51) Park, K.; Hayashi, T.; Tomiyasu, H.; Endo, M.; Dresselhaus, M. S. *J. Mater. Chem.* **2005**, *15*, 407−411.
(52) Li, Y.; Zhang, X.; Luo, J.; Huang, W.; Cheng, J.; Luo, Z.; Li, T.; Lui, F.; Xu, G.; Ke, X.; Li, L.; Geise, H. J. *Nanotechnology* **2004**, *15*, 1645−1649.
(53) Hiura, H.; Ebbesen, T. W.; Tanigaki, K. *Adv. Mater.* **1995**, *7*, (3), 275−276.
(54) Langley, L. A.; Fairbrother, D. H. *Carbon* **2007**, *45*, (1), 47−54.
(55) Langley, L. A.; Villanueva, D. E.; Fairbrother, D. H. *Chem. Mater.* **2006**, *18*, (1), 169−178.

at 175 mW. Autocorrelations were acquired for 15 s at a scattering angle of 90° and a 200 μm aperture. For each temporal measurement, the effective hydrodynamic diameter (D_h) of the particles in the dispersed O-MWCNT suspension was determined using a second-order cumulant function to model the autocorrelation function and solve the Stokes−Einstein equation.

For each O-MWCNT suspension studied, the initial hydrodynamic diameter ($D_{h(t=0)}$) prior to aggregation was determined. In these experiments, an aliquot of the O-MWCNT stock solution was first diluted with a predetermined volume of milli-Q water and vortex mixed for 1 s. The mixture was then inserted into the light scattering chamber and allowed to thermally equilibrate for 1 min. To precisely determine $D_{h(t=0)}$, 3 to 5 DLS measurements were performed. The vortex mixing was used to ensure that the O-MWCNTs were well mixed although sample analysis with and without vortex mixing gave the same answer.

To induce aggregation, a predetermined volume of 4 M NaCl was added to the diluted O-MWCNT stock solution. Although the NaCl concentration varied in each aggregation experiment, the predetermined volume of milli-Q water and 4 M NaCl added to the O-MWCNT stock solution was such that the initial particle concentration (N_0) of O-MWCNTs was held constant. Upon addition of the NaCl electrolyte solution, the mixture was vortex mixed for approximately 1 s and promptly reinserted into the analysis chamber, whereupon TR-DLS measurements were initiated. To ensure that data reflected O-MWCNT particles aggregating under the influence of Brownian motion, the first TR-DLS measurement taken after the vortex mixing was ignored. TR-DLS experiments proceeded until either the D_h exceeded 400 nm or 25 data points had been acquired. Measured values of $D_h \geq 800$ nm were excluded from analysis. These aberrant data points (<1% of all data acquired) were presumably due to residual dust particles or macroscopic aggregates entering the laser's scattering volume. All aggregation experiments were conducted in triplicate. It should be noted that in the absence of added electrolytes, all of the O-MWCNT suspensions used in TRDLS experiments remained stable for at least 2 weeks.

Analysis of TRDLS Data. The aggregation kinetics of O-MWCNTs were analyzed relative to the initial rate of aggregation as defined by eq 2,

$$\left(\frac{dD_h}{dt}\right)_{t\to 0} = \Theta k_a N_0 \quad (2)$$

where Θ is an instrumental constant that depends on the scattering angle and physical properties of the particles, N_0 is the initial concentration of particles in solution, and k_a is the initial rate constant for aggregation.[18−20,43,44,56] According to colloidal theory, at a fixed temperature and pH, the value of k_a depends upon the nature of the aggregating particles, as well as the valence and concentration of counterions. At sufficiently high electrolyte concentrations, particle aggregation rates become diffusion limited and $(dD_h/dt) = (dD_h/dt)_{fast}$. Experimentally, $(dD_h/dt)_{fast}$ was determined by averaging the 3 or 4 (dD_h/dt) values obtained in solution conditions where (dD_h/dt) remained constant, despite further increases in electrolyte concentration. (dD_h/dt) values measured at lower electrolyte concentrations (in the reaction-limited regime of aggregation) were then normalized to $(dD_h/dt)_{fast}$. Since the initial particle concentration (N_0) was constant for a given set of aggregation studies, eq 3 shows that $(dD_h/dt)/(dD_h/dt)_{fast}$ is equal to $k_a/k_{a,fast}$, which is also known as the aggregation attachment efficiency, α_A and is in effect a particle−particle sticking probability. α_A is also known as the inverse particle stability ratio (W^{-1}).[25,44]

$$\frac{(dD_h/dt)_{t\to 0}}{(dD_h/dt)_{t\to 0,fast}} = \frac{\Theta k_a N_0}{\Theta k_{a,fast} N_0} = \frac{k_a}{k_{a,fast}} = \frac{1}{W} = \alpha_A \quad (3)$$

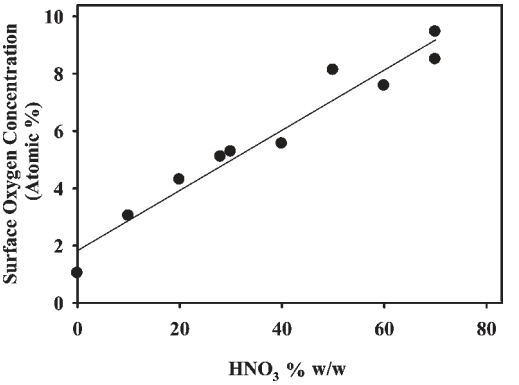

Figure 1. Influence of HNO_3 concentration on the surface oxygen concentration of O-MWCNTs.

As noted above, N_0 was held constant for all aggregation experiments involving a particular O-MWCNT. Although the value of N_0 does not need to be known to determine W^{-1}, based on the O-MWCNT suspension's absorbance at 500 nm (due to scattering) and using a previously measured extinction coefficient (ε_{500}) of 41 mL mg^{-1} cm^{-1}, N_0 was determined to be $\approx$ 0.75 mg/L. This is similar to values obtained by other researchers for MWCNTs particles suspended in solution.[57]

To determine the particle's colloidal stability, the calculated value of α_A (or W^{-1}) is plotted as a function of the counterion concentration [Na^+] used to induce aggregation, yielding a stability profile. Once constructed, the stability profile can be analyzed using eq 4.[25]

$$\frac{1}{W} = \frac{1}{1+(CCC/[Na^+])^\beta} \quad (4)$$

In this expression, β is d log(W^{-1})/d log ([Na^+]) in the regime where log (W^{-1}) $\propto$ log ([Na^+]). By fitting the stability profile with eq 4, the critical coagulation concentration (CCC) for each O-MWCNT can be obtained. The CCC is the minimum concentration of electrolyte needed to induce diffusion-limited aggregation and represents a useful metric of colloidal stability.

(III). Results and Discussion

The results and discussion are organized as follows: In the first section, we compare the chemical and physical properties (e.g., length, structure, surface composition, surface charge) of O-MWCNT powders, analyzed before and after different oxidative treatments. In the next section, we examine the chemical and physical properties of suspended O-MWCNT particles prepared in aqueous solution by prolonged (20 h) sonication of O-MWCNTs. In the final three sections, we report on and discuss the aggregation kinetics of different O-MWCNT particles in relationship to their surface properties.

Characterization of O-MWCNTs Powders. The extent of oxygen incorporation into the MWCNT's surface was sensitive to both the oxidant used and the reaction conditions. For example, the extent of surface oxygen incorporation (measured by XPS) exhibited an approximately linear dependence on the HNO_3 concentration between 0 to 70% w/w as shown in Figure 1. In comparison, O-MWCNTs prepared by refluxing the pristine nanomaterials with H_2SO_4/HNO_3 exhibited an intermediate surface oxygen concentration (6.1%), while O-MWCNTs prepared from H_2SO_4/HNO_3 in a microwave displayed a significantly higher concentration of surface oxygen (10.8%). MWCNTs

(56) Holthoff, H.; Egelhaaf, S. U.; Borkovec, M.; Schurtenberger, P.; Sticher, H. *Langmuir* **1996**, *12*, 5541−5549.

(57) Li, Z. F.; Luo, G. H.; Zhou, W. P.; Wei, F.; Xiang, R.; Liu, Y. P. *Nanotechnology* **2006**, *17*, 3692−3698.

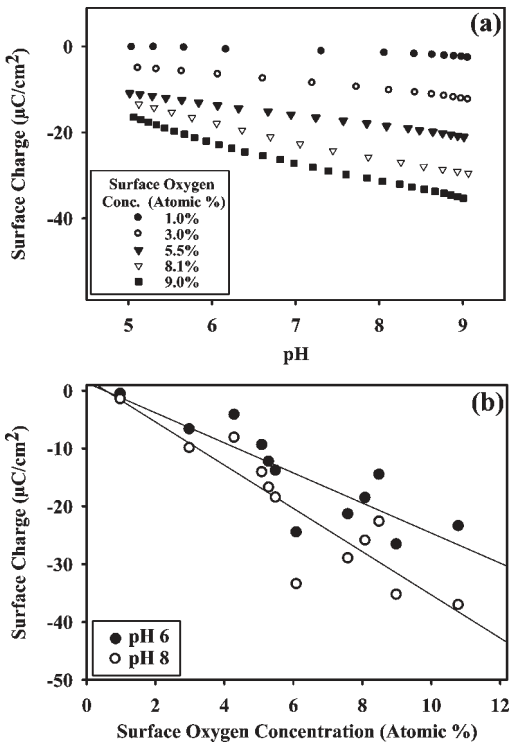

Figure 2. (a) Surface charge density of O-MWCNTs with different surface oxygen concentrations, measured as a function of pH. (b) Influence of surface oxygen concentration on the surface charge of O-MWCNTs at pH 6 and 8. All measurements were conducted in the presence of ~64 mM NaCl.

oxidized with $KMnO_4$ displayed a surface oxygen concentration of 9.0%. For reference, the surface oxygen concentration of pristine MWCNTs was < 2%.

The surface charge of O-MWCNT powders was found to depend on the level of oxidation and pH. Figure 2a illustrates that while the pristine MWCNTs remained essentially neutral over the pH range between 5 and 9, the surface charge on O-MWCNTs increased in magnitude systematically as the level of surface oxygen increased. O-MWCNTs that exhibited higher concentrations of surface oxygen displayed a greater rate of increase in surface charge (measured by the gradients in Figure 2a with increasing pH. The results shown in Figure 2b also illustrate that, over the range of pH values studied, the surface charge on the O-MWCNTs is proportional to the surface oxygen concentration. For example at pH 6, we observed the following relationship:

$$\text{Surface charge}(\mu\text{C/cm}^2) = (\text{Surface oxygen concentration} \times -0.34) + 2.2 \ (R^2 = 0.89)$$

It should be noted that although the above equation has been established for the MWCNTs used in the present study, additional studies are needed to assess the extent to which the nature of the correlation depends upon the type of CNT under investigation.

Compared to metal oxides[58] the surface charge of our oxidized MWCNTs is high. However, when compared to the surface charge density of graphite oxide (oxidized graphene sheets, similar to the CNTs' surface) our results are quite similar: For our O-MWCNTs the surface charge density (charge/nm^2) ranges from 0.03 to 1.4 at pH 6. Similarly, the surface charge density of graphite oxide (GO) ranges from 0.001 to 1.4[59−61]

In addition to chemical changes, the physical properties of CNTs could be changed by aggressive oxidizing conditions.[62] In prior studies, we have used TEM, AFM, and BET surface-area analysis to compare the physical properties of pristine and O-MWCNT powders.[30] Results from these prior TEM and AFM studies showed that oxidation produced no systematic changes in the structural integrity or length distribution of the O-MWCNTs compared to the pristine nanomaterial. In these previous studies, AFM and TEM analyses of O-MWCNT powders were conducted after they were dispersed in Milli-Q water, although the sonication time was limited to 15 min (in contrast to the 20 h used to create colloidally dispersed O-MWCNTs) to minimize any unwanted effects of sonication on the O-MWCNT length distribution. Analogous to our previous TEM and AFM data, BET measurements revealed that the surface areas of almost all O-MWCNTs were within 15 m^2/g of the BET SA of the pristine MWCNTs (265 m^2/g). The exceptions were the O-MWCNTs prepared by refluxing in H_2SO_4/HNO_3 (210 m^2/g) and with $KMnO_4$ (304 m^2/g).

To further characterize the O-MWCNTs, Raman spectroscopy (performed at λ = 514 nm) was conducted (see Supporting Information, Table S2). It should be noted that while Raman is a valuable tool for characterizing the purity of SWCNTs, it less useful for MWCNTs because the radial breathing modes are too weak to be observed.[63,64] Raman spectra indicated, nonetheless, that the I_D/I_G band ratio for O-MWCNTs typically exhibited an increase compared with the pristine nanomaterials, consistent with an increase in structural disorder caused by the sidewall damage that accompanies oxidation. The one exception was the MWCNTs oxidized with $\mu\lambda/H_2SO_4/HNO_3$. In this case, the I_D/I_G ratio decreased in comparison to the pristine nanomaterials.

Characterization of Colloidal O-MWCNTs. As described in the Experimental Section, colloidal suspensions of O-MWCNTs were created by dispersing measured quantities of O-MWCNT powders in Milli-Q water using a sonication time of 20 h. Since energy imparted during sonication has the potential to change the chemical composition of the O-MWCNTs,[65] a control study was performed to investigate the effect of sonication on the surface composition of O-MWCNTs. XPS results indicated that sonication produced no measurable change in the surface oxygen concentration (±0.2%).

To probe the structure and aggregation state of O-MWCNT colloids, a select number of suspensions were examined using TEM and AFM. Figure 3 shows an illustrative example of a low and high-magnification TEM image of O-MWCNT particles deposited from colloidal suspensions onto a holey-carbon grid. The low-magnification image clearly shows the structure of the holey-carbon grid, as well as the rod-like nanotubes, while the high-magnification image emphasizes a single MWCNT's fine structure (i.e., hollow interior and multiple graphene layers). Close inspection of the high-magnification TEM image reveals

(58) Larson, I.; Attard, P. *J. Colloid Interface Sci.* **2000**, *227*, (1), 152−163.
(59) Szabó, T.; Tombácz, E.; Illés, E.; Dékány, I. *Carbon* **2006**, *44*, (3), 537−545.
(60) Cassagneau, T.; Guerin, F.; Fendler, J. H. *Langmuir* **2000**, *16*, (18), 7318−7324.
(61) Kotov, N. A.; Dékány, I.; Fendler, J. H. *Adv. Mater.* **1996**, *8*, (8), 637−641.
(62) Rosca, I. D.; Watari, F.; Uo, M.; Akasaka, T. *Carbon* **2005**, *43*, 3124−3131.
(63) Murphy, H.; Papakonstantinou, P.; Okpalugo, T. I. T. *J. Vac. Sci. Technol. B* **2006**, *24*, (2), 715−720.
(64) Osswald, S.; Havel, M.; Gogotsi, Y. *J. Raman Spectrosc.* **2007**, *38*, 728−736.
(65) Yang, D.-Q.; Rochette, J.-F.; Sacher, E. *J. Phys. Chem. B* **2005**, *109*, 7788−7794.

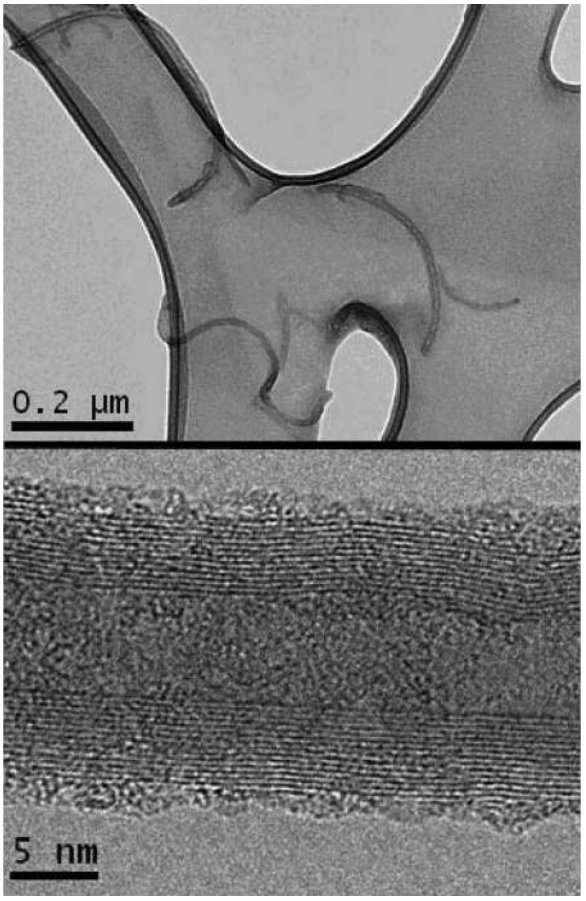

Figure 3. (Top) Low and (Bottom) hi-magnification TEM micrographs of O-MWCNTs refluxed in 70% w/w HNO_3 and then sonicated for 20 h to form a colloidal suspension.

patches of disordered carbon at the MWCNT's surface. Figure 3 also highlights the fact that even though O-MWCNTs were dried onto the carbon grid from solution, individual O-MWCNT particles were still observed, suggesting that sonication produces suspensions containing individual nanoparticles. This assertion is supported by AFM data, where the overwhelming majority of the colloidal O-MWCNT particles, flash dried onto Si substrates, were imaged as individual rod-like structures with a modest degree of curvature (see Supporting Information, Figure S1). Occasionally ring-like structures were observed, presumably because of drying effects.

The fact that individual MWCNTs could be resolved by AFM enabled us to compare the length distribution of colloidally dispersed O-MWCNTs (formed by sonicating O-MWCNT powders in Milli-Q water for 20 h) that exhibited different surface oxygen concentrations. Results from this analysis are shown in Figure 4 for three O-MWCNTs that possessed low (4.3%), intermediate (8.1%), and high (9.5%) concentrations of surface oxygen. In each case, AFM analysis was based on 1,000 measurements of individual O-MWCNTs. As a function of increasing surface oxygen concentration, the O-MWCNTs exhibited length distributions of 0.5 ± 0.3 μm, 0.7 ± 0.5 μm, and 0.5 ± 0.4 μm. A more comprehensive statistical analysis of the O-MWCNT length distributions measured by AFM can be found in Supporting Information, Table S3. Complementary statistical TEM analysis conducted on O-MWCNTs having 9.5% surface oxygen revealed an average length distribution of 0.4 ± 0.4 μm (based on 125 measurements), consistent with the AFM results. Collectively, these AFM and TEM results demonstrate that there

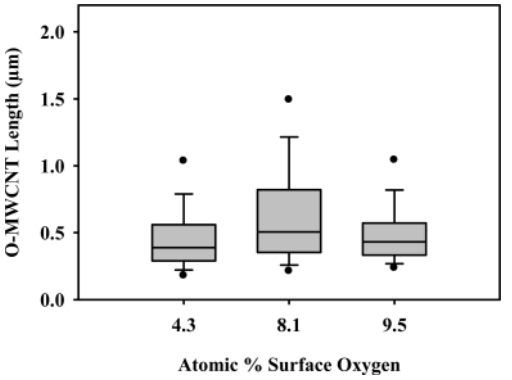

Figure 4. Box plots illustrating the length distributions of three O-MWCNT suspensions. Each suspension contained O-MWCNTs with a different concentration of surface oxygen.

was no systematic variation or significant differences in the length distributions of suspended O-MWCNT particles as a function of their surface oxygen concentration. It should be noted, however, that the length distribution of colloidally dispersed O-MWCNTs (≈ 0.5 μm) are in marked contrast to the 5−20 μm lengths quoted by the manufacturer for the pristine MWCNTs. This shortening of O-MWCNTs, that results from the prolonged periods of sonication (20 h) required to create colloidally stable dispersions in Milli-Q water, is consistent with observations reported in previous studies of MWCNT and SWCNTs.[66]

In summary, our results demonstrated that different oxidative methods can be used to generate colloidal suspensions containing O-MWCNTs particles with different levels of surface oxygen but comparable length distributions. Thus, *differences in the colloidal stability of the O-MWCNTs can be ascribed to the effects of surface oxygen.*

For colloidal particles, electrophoretic mobility (EM) is often used as a metric of surface potential.[67] Previously, we have shown that O-MWCNT particles exhibit negative EMs, with a magnitude that decreased as the electrolyte concentration increased, consistent with the behavior expected for colloidal particles with a net negative charge.[48] The influence of surface oxygen concentration and pH on the EM of colloidal O-MWCNT particles is illustrated in Figure 5. Results from these studies revealed that EM values increased as pH was increased from 4 to 6, irrespective of the level of surface oxidation. However, at pH values greater than 6, little or no change in the EM was observed for any of the O-MWCNTS studied. These observations on the influence of pH on the EM of acid washed/O-MWCNTs are consistent with previous research.[68,69] As a function of surface oxygen concentration (at a constant electrolyte composition), Figure 5 also reveals that there is little or no systematic pH dependence in the EM of different O-MWCNTs, in marked contrast to the clear pH dependence observed for surface charge (see Figure 2(b)).

Influence of Surface Oxygen Concentration on the Aqueous Colloidal Stability of O-MWCNTs. A qualitative assessment of the role that surface oxygen plays in moderating the aquatic stability of O-MWCNTs is provided in Figure 6. The

(66) Hennrich, F.; Krupke, R.; Arnold, K.; Rojas Stuetz, J. A.; Lebedkin, S.; Koch, T.; Schimmel, T.; Kappes, M. M. *J. Phys. Chem. B* **2007**, *111*, (8), 1932−1937.
(67) Evans, D. F.; Wennerström, H. *The Colloidal Domain. Where Physics, Chemistry, and Biology Meet*. 2nd ed.; John Wiley & Sons, Inc.: New York, 1999; pp 1−632.
(68) Esumi, K.; Ishigami, M.; Nakajima, A.; Sawada, K.; Honda, H. *Carbon* **1996**, *34*, 279−281.
(69) Hu, H.; Yu, A.; Kim, E.; Zhao, B.; Itkis, M. E.; Bekyarova, E.; Haddon, R. C., *J. Phys. Chem. B* **2005**, *109*, 11520−11524.

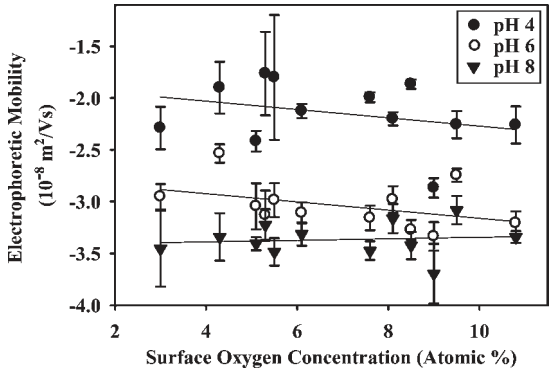

Figure 5. Electrophoretic mobility of O-MWCNTs as a function of surface oxygen concentration, measured at pH 4,6, and 8. All measurements were performed in the presence of ~64 mM NaCl.

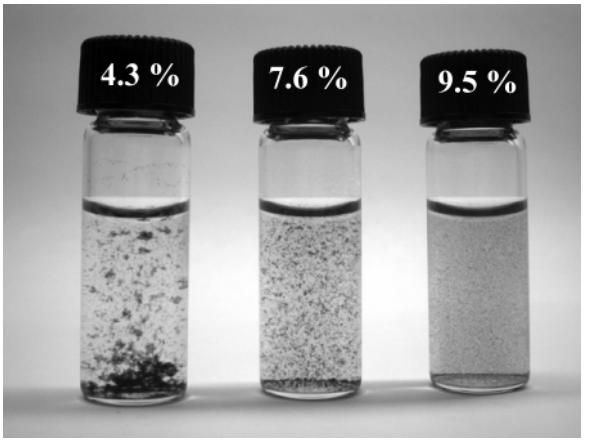

Figure 6. Influence of surface oxygen concentration on the perikinetic aggregation of O-MWCNTs (7.5 mg/L) These experiments were performed at pH 6 in the presence of 64 mM NaCl. Aggregation was allowed to proceed for 120 min. The O-MWCNT surface oxygen concentration determined by XPS is indicated on the cap of each vial.

experimental results illustrated in Figure 6 were obtained using three initially stable suspensions of O-MWCNTs (7.5 mg O-MWCNT/L), that differed in their extent of surface oxidation (shown on the cap of each vial). Each suspension was prepared at pH 6. To induce aggregation in each vial, the ionic strength was increased to 64 mM by adding an appropriate aliquot of 4 M NaCl. Perikentic aggregation was then allowed to proceed for 120 min. Clearly, the extent of aggregation was dependent upon the O-MWCNTs' surface oxygen concentration: large settleable aggregates had formed for O-MWCNTs containing 4.3% surface oxygen, while significantly smaller aggregates were observed in the solution containing O-MWCNTs with 7.6% surface oxygen. For O-MWCNTs with 9.5% surface oxygen, aggregates were barely visible.

Using TR-DLS to monitor changes in D_h, more quantitative information was acquired on the influence that surface oxygen exerts on the colloidal stability of O-MWCNTs. Aggregation profiles of the same three O-MWCNTs shown in Figure 6 were measured under the same solution conditions (pH 6.0 and 64 mM NaCl). However, to reduce the aggregation rate so that the change in D_h could be accurately monitored over the course of several minutes, the concentration of O-MWCNTs was reduced to 0.75 mg MWCNT/L. Results from these experiments, shown in Figure 7, revealed that irrespective of the level of surface

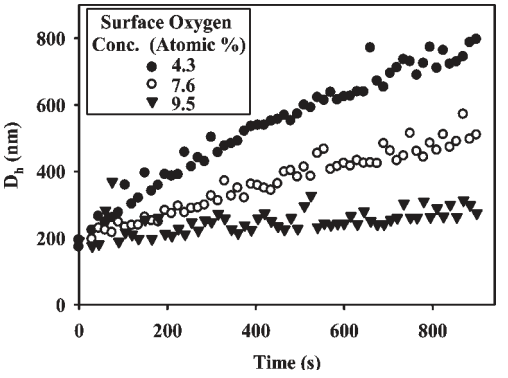

Figure 7. Influence of surface oxygen concentration on the aggregation profiles of O-MWCNTs. Each experiment was obtained at an O-MWCNT concentration of ~0.75 mg/L in the presence of 64 mM NaCl at pH 6.

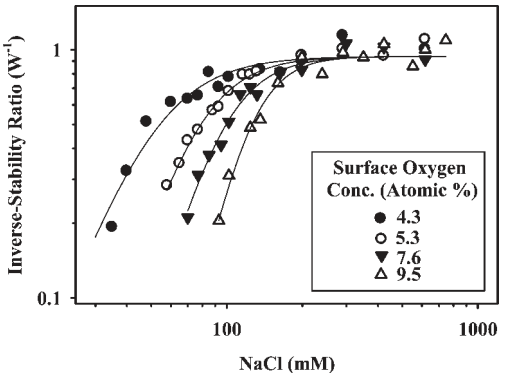

Figure 8. Influence of surface oxygen concentration on the stability profiles of O-MWCNTs (~0.75 mg/L) as a function of NaCl concentration, at pH 6.

oxidation, the effective hydrodynamic diameter of the suspended O-MWCNT particles before aggregation ($D_{h(t=0)}$) was ≈ 200 nm. This result agrees qualitatively with the AFM data shown in Figure 4 which indicated that the particle-size distribution was independent of the surface oxygen concentration. The aggregation rates inferred from the data shown in Figure 7 exhibit a systematic dependence upon the extent of MWCNT surface oxidation, consistent with the results shown in Figure 6. Thus, for MWCNTs that contained 9.5% surface oxygen, the D_h increased by approximately 50% over the 900 s of aggregation time. In contrast, over the same time period, the D_h for MWCNTs that contained 7.6% and 4.3% oxygen increased by approximately 170 and 350%, respectively. The results presented in Figure 7 also highlight the fact the initial rate of O-MWCNTs aggregation can be described by a linear increase in D_h as a function of time. This behavior is analogous to that observed for spherical particles, and allowed us to analyze the particle stability profiles using eqs 2, 3, and 4, as detailed in the Experimental Section.

Stability profiles, collected at pH 6 for a selected number of O-MWCNTs, are shown in Figure 8. Each stability profile exhibits both reaction-limited and diffusion-limited aggregation regimes, consistent with the precepts of DLVO theory.[47−49] Furthermore, reaction-limited aggregation was observed over a wider range of electrolyte concentrations as the surface oxygen concentration on the O-MWCNT increased. This indicates that more oxidized O-MWCNTs will remain mobile in aquatic environments over a wider range of solution conditions.

Table 1. Influence of Surface Oxide Distribution on the Colloidal Stability of O-MWCNTs

			functional group conc. (atomic %)			
sample	surface oxygen concentration (atomic %)	CCC (mM NaCl)	COOH	C−OH	C=O	other oxides
O-MWCNT(A) before heat treatment	12.8	128	7.9	1.9	2.7	0.4
O-MWCNT(A) after heat treatment	4.7	unstable suspension	1.3	1.3	1.8	0.2
O-MWCNT(B)	4.3	55	1.9	0.8	0.9	0.6

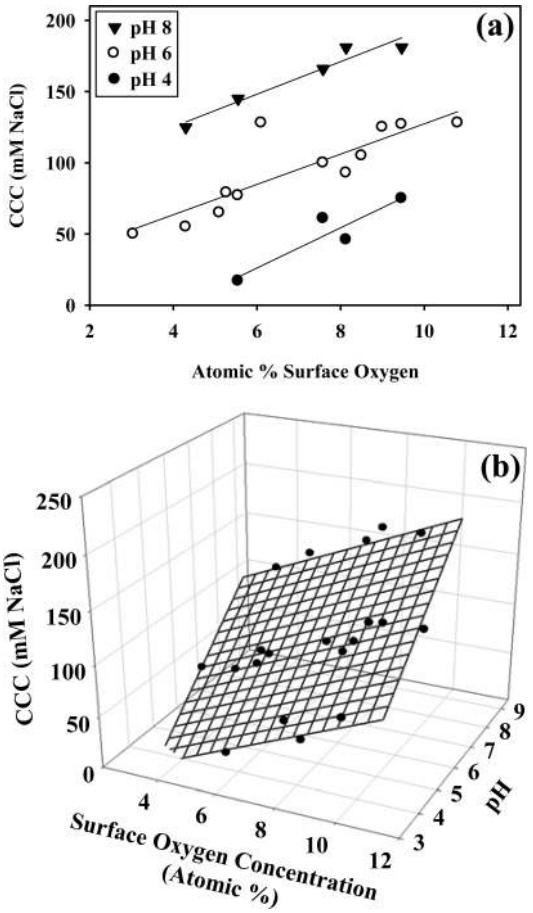

Figure 9. (a) Influence of surface oxygen concentration on the critical coagulation concentration (CCC) of O-MWCNTs at pH 4,6, and 8. (b) Three-dimensional plot showing the functional interdependence of surface oxygen concentration, pH, and CCC of O-MWCNTs.

For each O-MWCNT studied, aggregation profiles could be well described by eq 4. Fits to eq 4 are shown as solid lines in Figure 8 with R^2 values in the range of 0.93 to 0.99. The various CCCs obtained by these model fits provided a quantitative metric of the colloidal stability for each O-MWCNT. In Figure 9a, the CCC for each O-MWCNT is plotted as a function of surface oxygen concentration. Additional data, shown for O-MWCNT suspensions studied at pH 4, 6, and 8 are also shown. These plots clearly show that for the vast majority of the O-MWCNTS studied, the *CCC exhibits a linear dependence on the surface oxygen concentration* over the full range of pH values studied (4−8). The one exception is the O-MWCNTs prepared by refluxing MWCNTs in H_2SO_4/HNO_3, which exhibited a significantly higher CCC than would have been predicted on the basis of their surface oxygen concentration. Analysis of Figure 9a also shows that for a given concentration of surface oxygen, the colloidal stability of O-MWCNTs increases with increasing pH. This is consistent with a previous study that focused on the influence of solution conditions on the colloidal stability of an acid-washed MWCNT.[48] To analyze the combined effects of pH, surface oxygen concentration, and CCC, a three-dimensional plot of the data shown in Figure 9a is presented in Figure 9b. This rendering shows that particle stability is coplanar with respect to these variables.[70] The existence of such a "critical plane" indicates that the colloidal stability of the majority of O-MWCNTs in aqueous environments can be predicted if the pH of the solution and the surface composition of the O-MWCNTs are both known. The range of aquatic conditions over which O-MWCNTs are expected to remain colloidally stable will also depend on the electrolyte composition since the behavior of O-MWCNT particles has been shown to adhere to the Schultz−Hardy rule, which predicts that CCC $\propto Z^{-6}$, where Z is the counterion valence.[48,49]

Influence of Oxygen Containing Functional Groups on the Colloidal Stability of O-MWCNTs. The surface oxygen signal measured by XPS can be further characterized in terms of the distribution of different oxygen containing functional groups (e.g., hydroxyl, carbonyl groups) present on the MWCNT surface. To better understand the relative importance that these different surface oxides play in determining the colloidal stability of O-MWCNTs, we have used chemical derivatization in conjunction with XPS to quantify the distribution of oxygen-containing functional groups on different O-MWCNTs. Consistent with previous spectroscopic studies of oxidized MWCNTs, our chemical derivatization results confirm the presence of hydroxyl, carbonyl, and carboxylic acid groups.[71−74] An example of the distribution of oxygen-containing functional groups on O-MWCNTs, created by oxidizing in H_2SO_4/HNO_3, is shown in Table 1. These results are consistent with prior data that indicates that carboxylic acid groups are the surface oxides present in the highest concentration.[72]

Information on the distribution of surface oxides enabled us to examine the functional relationship between the CCC of O-MWCNTs (measured at pH 6) and the concentration of each functional group.[70] Results from this analysis revealed that the CCC of O-MWCNTs was most closely correlated with the carboxylic acid group concentration ($R^2 = 0.72$, as shown in Figure 10a), with significantly poorer correlations for both hydroxyl and carbonyl groups (R^2 values were 0.07 and 0.46 respectively, data shown in the Supporting Information, Figure S2).[70] The important role that carboxylic-acid groups play in determining the colloidal stability of O-MWCNTs can be ascribed to the fact that among the different surface oxides, carboxylic acid groups are the only ones deprotonated at pH 6 and therefore carry a negative charge.

To explicitly demonstrate that the oxide distribution plays an important role in determining the O-MWCNTs′ colloidal stability, we compared the aqueous stability of two O-MWCNTs that

(70) This analysis precludes the O-MWCNTs prepared by refluxing MWCNTs in H_2SO_4-HNO_3. These O-MWCNTs exhibited a markedly higher CCC than would have been predicted on the basis of their surface oxygen concentration.

(71) Zhang, N.; Xie, J.; Varadan, V. K. *Smart Mater. Struct.* **2002**, *11*, 962−965.
(72) Blanchard, N. P.; Hatton, R. A.; Silva, S. R. P. *Chem. Phys. Lett.* **2007**, *434*, 92−95.
(73) Banerjee, S.; Wong, S. S. *J. Phys. Chem. B* **2002**, *106*, (47), 12144−12151.
(74) Simmons, J. M.; Nichols, B. M.; Baker, S. E.; Marcus, M. S.; Castellini, O. M.; Lee, C.-S.; Hamers, R. J.; Eriksson, M. A. *J. Phys. Chem. B* **2006**, *110*, 7113−7118.

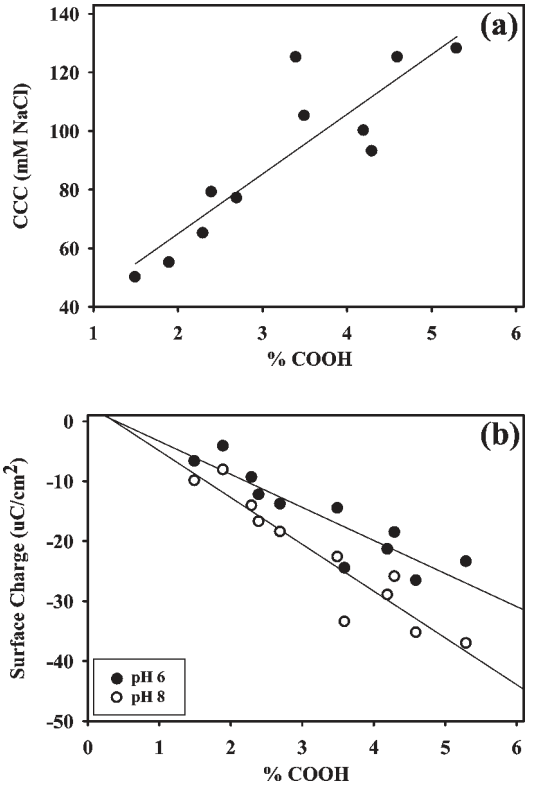

Figure 10. Influence of carboxylic-acid group concentration on (a) the CCC measured at pH = 6, and (b) the surface charge measured at pH 6 and 8.

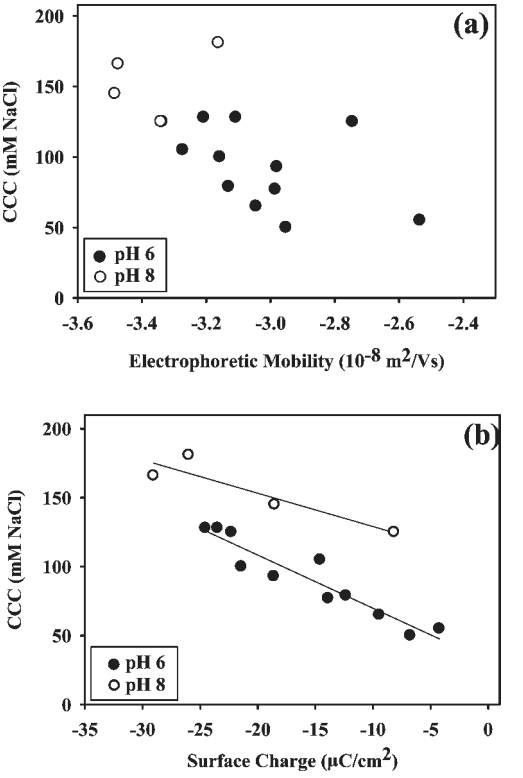

Figure 11. Relationship between (a) the CCC and surface charge of O-MWCNTs; (b) the CCC and the electrophoretic mobility of O-MWCNTs. In both (a) and (b), measurements were taken at pH 6 and 8, in the presence of ~64 mM NaCl.

exhibit a comparable total oxygen concentration but drastically different distributions of oxygen-containing functional groups. To produce an O-MWCNT with a significantly different oxide distribution, an acid washed O-MWCNT that contained an initially high surface oxygen concentration (O-MWCNT's (A) Before Heat Treatment in Table 1) was heated to 500 °C, under argon, for 12 h. XPS data on this heat-treated O-MWCNT showed that, upon heating, the surface oxygen concentration decreased from 12.8% to 4.7%. XPS performed in conjunction with chemical derivitization indicated that this decrease in oxygen concentration because of heating was principally due to decarboxylation of the native carboxylic acid groups, while most of the hydroxyl and carbonyl groups remained intact (see Table 1). TEM data indicated that these heat-treated O-MWCNTs (O-MWCNT's (A) After Heat Treatment in Table 1) remain structurally intact (see Supporting Information, Figure S3). After the sonication period (20 h) used to create colloidal suspensions of O-MWCNTs, the heat treated O-MWCNTs did not form a stable suspension at pH 6. In contrast, acid washed O-MWCNTs that exhibited a slightly *lower total oxygen concentration* (4.3%) but a *higher concentration of carboxyl groups* did form a stable colloidal suspension (O-MWCNT(B) in Table 1). This result reinforces the idea that carboxylic-acid groups are particularly important in regulating colloidal stability. This assertion is also supported by surface charge data which showed that at environmentally relevant pH(4−7) conditions, the furnace treated O-MWCNTs (O-MWCNT's (A) After Heat Treatment in Table 1) have behavior comparable to that of the pristine nanomaterials despite the presence of 4.7% total surface oxygen.

Nonetheless, oxygen-containing functional groups other than carboxylic acids also contribute to the colloidal stability of O-MWCNTs. This assertion is indicated by the fact that the colloidal stability is better correlated with the overall oxygen concentration (Figure 9a), rather than the carboxylic acid group concentration, alone (Figure 10a). This is not surprising given the energetically favorable interactions (hydrogen-bonding) that can exist between water molecules and hydroxyl groups, carbonyl groups, and "other oxides" (e.g., esters and ethers) whose concentration cannot be assayed with chemical derivitization.

Influence of Other Surface Properties (Charge and Electrophoretic Mobility) on the Colloidal Stability of O-MWCNTs. In addition to surface chemistry, other surface properties such as electrophoretic mobility and surface charge may also be useful in rationalizing differences in the colloidal stability of O-MWCNTs. If correlations with these properties could be established, they would provide a more convenient route to make evaluations and predictions. To directly compare surface charge and electrophoretic-mobility measurements obtained on different O-MWCNTs, experiments were performed at the same electrolyte concentration (64 mM NaCl). Figure 5 reveals that no discernible correlation exists between the surface oxygen concentration and the electrophoretic mobility of O-MWCNTs over the range of pH values studied. Consequently, there was no correlation between electrophoretic mobility and the colloidal stability of O-MWCNTs (Figure 11a).[70] Similar results have been noted in previous studies, where researchers have observed that electrophoretic mobility of O-MWCNTs remains constant with increasing pH above pH 6,[69] even though the particles' colloidal stability continues to increase.[75] The underlying cause for this lack of correlation is unclear, but may be due to the fact that EM measures the charge density at the "zeta" plane, which is affected by a dynamic hydration shell including a layer of dissolved-phase counterions.

(75) Shieh, Y.-T.; Liu, G.-L.; Wu, H.-H.; Lee, C.-C. *Carbon* **2007**, *43*, 1880−1890.

In contrast to the electrophoretic mobility, surface charge is well correlated with surface oxygen, as shown by the data in Figure 2, panels a and b. Furthermore, Figure 11b shows that for O-MWCNTs at pH 6 and 8 the CCC, and thus the colloidal stability, increases linearly with increasing surface charge.[70] These results are also consistent with the basic precepts of DLVO theory, which predict that more negatively charged O-MWCNT particles should remain colloidally stable over a wider range of solution conditions. The mathematical relationship between the CCC and surface charge, however, is also dependent upon pH. Thus, the surface charge and the pH must both be known to predict the colloidal stability of the O-MWCNTs. This is consistent with the interdependence observed between surface oxygen concentration, CCC and pH (Figure 9, panels a and b).

At a molecular level, the monotonic increase in surface charge under acidic conditions (pH < 6) can be ascribed to the deprotonation of carboxylic acid groups. This is supported by the linear correlations observed between surface charge and the concentration of carboxylic acid groups, measured at pH 6 (see Figure 10b). In contrast, much poorer correlations were observed between surface charge and the concentration of either carbonyl or hydroxyl groups (see Supporting Information, Figure S4). The role of functional groups other than carboxylic acid groups is suggested by the continued increase in surface charge above pH 6 (Figure 2a), where all carboxylic acid groups should be deprotonated. Increases in surface charge at higher pH values have also been observed on other types of carbonaceous materials and may originate from either the deprotonation of acid sites, such as a phenolic −OH group, or the neutralization of positively charged basic sites.[76] The source of such basic surface sites on carbonaceous materials remains poorly understood, but may include the π electrons associated with the CNT's graphene surface or pyrone-based oxygen functional groups.[77,78] Indeed, the origin of negative charges on many nanomaterials in suspension remains unclear.

A number of additional questions arise from this study, and follow-up studies are needed to explore the extent to which predictive models can be developed to include the effects of (i) other commonly used oxidative methods not studied as part of this investigation (e.g., ozonolysis,[79] hydrogen peroxide), (ii) surface oxygen on the colloidal stability of other types of carbon based nanomaterials such as SWCNTs and fullerenes, and (iii) other chemical modification strategies (e.g., amination) that are also capable of creating colloidal suspensions of CNTs. Another issue is the role that dissolved natural organic matter will have on the colloidal stability of O-MWCNTs.

(76) Bjelopavlic, M.; Newcombe, G.; Hayes, R. *J. Colloid Interface Sci.* **1999**, *210*, 271−280.
(77) Boehm, H. P. *Carbon* **2002**, *40*, (2), 145−149.
(78) Fuente, E.; Menendez, J. A.; Suarez, D.; Montes-Moran, A. *Langmuir* **2003**, *19*, (8), 3505−3511.
(79) Li, M.; Boggs, M.; Beebe, T. P.; Huang, C. P. *Carbon* **2008**, *46*, 466−475.

(IV). Conclusions

The extent of oxygen incorporation into the surface of multiwalled carbon nanotubes (MWCNTs) is dependent upon the oxidizing agents and reaction conditions used to treat/functionalize this engineered nanomaterial. Comparatively small changes in surface oxygen concentration have been shown to provoke significant changes in the aqueous colloidal stability of O-MWCNTs. Functional relationships were observed between the concentration of surface oxygen, the surface charge, and the aqueous colloidal stability of oxidized MWNCTs (O-MWCNTs) under pH conditions commonly found in the environment. In contrast, correlations between colloidal stability and electrophoretic mobility were very poor. The distribution of oxygen-containing functional groups on the surface of O-MWCNTs also influences the particle's colloidal stability, with carboxylic-acid groups playing the dominant role. The overarching conclusion of this study is that changes in a nanoparticle's surface composition lead to predictable changes in phenomenological properties, such as particle stability. Consequently, structure−property relationships can be established to help understand and predict not only the behavior of these particles but also the health and safety risks they pose.

Acknowledgment. The authors gratefully acknowledge financial support from the National Science Foundation (Grant # BES0731147), the Environmental Protection Agency (Grant # RD-83385701-0), the Institute for Nanobiotechnology at Johns Hopkins University, and the ARCS Foundation Inc. We would like to acknowledge Professor Charlie O'Melia (Department of Geography and Environmental Engineering, Johns Hopkins University) for scientific discussions, insight, and allowing us to use the DLS apparatus and potentiometric titration system. The authors would also like to acknowledge the Material Science Department at JHU for use of the surface analysis laboratory. We would also like to acknowledge Amanda Bertele (College of Notre Dame, Baltimore, MD) for her assistance in preparing and cleaning the O-MWCNTs. We would also like to acknowledge Yo-Rhin Rhim (Department of Mechanical Engineering, Johns Hopkins University, Baltimore MD) for collecting the Raman data.

Supporting Information Available: BET surface areas for O-MWCNTs prepared with HNO_3, H_2SO_4/HNO_3 and $KMnO_4$ (Table S1). Raman data showing the I_D/I_G band ratios for pristine and oxidized MWCNTs (Table S2). Additional length statistics for O-MWCNTs measured with AFM (Table S3). Representative AFM image used to acquire MWCNT length distributions (Figure S1). Correlations between the O-MWCNTs' CCC and corresponding hydroxyl and carbonyl group concentrations (Figure S2). TEM micrograph of furnace treated O-MWCNTs (Figure S3). Effect of hydroxyl and carbonyl groups on the O-MWCNTs' surface charge (Figure S4). This material is available free of charge via the Internet at http://pubs.acs.org.